ORIGINAL RESEARCH

Intracoronary Administration of Allogeneic Adipose Tissue–Derived Mesenchymal Stem Cells Improves Myocardial Perfusion But Not Left Ventricle Function, in a Translational Model of Acute Myocardial Infarction

Joaquim Bobi, DVM;* Núria Solanes, DVM, PhD;* Rodrigo Fernández-Jiménez, MD, PhD; Carlos Galán-Arriola, DVM; Ana Paula Dantas, PhD; Leticia Fernández-Friera, MD, PhD; Carolina Gálvez-Montón, DVM, PhD; Elisabet Rigol-Monzó, BPharm; Jaume Agüero, MD, PhD; José Ramírez, MD, PhD; Mercè Roqué, MD, PhD; Antoni Bayés-Genís, MD, PhD; Javier Sánchez-González, PhD; Ana García-Álvarez, MD, PhD; Manel Sabaté, MD, PhD; Santiago Roura, PhD; Borja Ibáñez, MD, PhD; Montserrat Rigol, DVM, PhD

Background—Autologous adipose tissue–derived mesenchymal stem cells (ATMSCs) therapy is a promising strategy to improve post–myocardial infarction outcomes. In a porcine model of acute myocardial infarction, we studied the long-term effects and the mechanisms involved in allogeneic ATMSCs administration on myocardial performance.

Methods and Results—Thirty-eight pigs underwent 50 minutes of coronary occlusion; the study was completed in 33 pigs. After reperfusion, allogeneic ATMSCs or culture medium (vehicle) were intracoronarily administered. Follow-ups were performed at short (2 days after acute myocardial infarction vehicle-treated, n=10; ATMSCs-treated, n=9) or long term (60 days after acute myocardial infarction vehicle-treated, n=7; ATMSCs-treated, n=7). At short term, infarcted myocardium analysis showed reduced apoptosis in the ATMSCs-treated animals (48.6±6% versus 55.9±5.7% in vehicle; P=0.017); enhancement of the reparative process with up-regulated vascular endothelial growth factor, granulocyte macrophage colony-stimulating factor, and stromal-derived factor-1α gene expression; and increased M2 macrophages (67.2±10% versus 54.7±10.2% in vehicle; P=0.016). In long-term groups, increase in myocardial perfusion at the anterior infarct border was observed both on day-7 and day-60 cardiac magnetic resonance studies in ATMSCs-treated animals, compared to vehicle (87.9±28.7 versus 57.4±17.7 mL/min per gram at 7 days; P=0.034 and 99±22.6 versus 43.3±14.7 22.6 mL/min per gram at 60 days; P=0.0001, respectively). At day 60, higher vascular density was detected at the border zone in the ATMSCs-treated animals (118±18 versus 92.4±24.3 vessels/mm^2 in vehicle; P=0.045). Cardiac magnetic resonance–measured left ventricular ejection fraction of left ventricular volumes was not different between groups at any time point.

Conclusions—In this porcine acute myocardial infarction model, allogeneic ATMSCs-based therapy was associated with increased cardioprotective and reparative mechanisms and with better cardiac magnetic resonance–measured perfusion. No effect on left ventricular volumes or ejection fraction was observed. **(*J Am Heart Assoc*. 2017;6:e005771. DOI: 10.1161/JAHA.117.005771.)**

Key Words: adipose tissue-derived mesenchymal stem cells • allogeneic origin • myocardial infarction • myocardial perfusion • vascular density

From the August Pi i Sunyer Biomedical Research Institute (IDIBAPS), Institut de Malalties Cardiovasculars, Hospital Clínic de Barcelona, Universitat de Barcelona, Spain (J.B., N.S., A.P.D., M.R., A.G.-Á., M.S., M.R.); Centro Nacional de Investigaciones Cardiovasculares Carlos III, CNIC, Madrid, Spain (R.F.-J., C.G.-A., L.F.-F., J.A., A.G.-Á., B.I.); Icahn School of Medicine at Mount Sinai, New York, NY (R.F.-J.); Hospital Universitario HM Montepríncipe, Madrid, Spain (L.F.-F.); ICREC Research Program, Health Science Research Institute Germans Trias i Pujol, Badalona, Spain (C.G.-M., A.B.-G., S.R.); Servei d'Immunologia (E.R.-M.) and Servei d'Anatomia Patològica (J.R.), Hospital Clínic de Barcelona, Barcelona, Spain; Cardiology Service, Germans Trias i Pujol University Hospital, Badalona, Spain (A.B.-G.); Department of Medicine, Universitat Autònoma de Barcelona (UAB), Barcelona, Spain (A.B.-G.); Philips Healthcare, Madrid, Spain (J.S.-G.); Center of Regenerative Medicine in Barcelona, Barcelona, Spain (S.R.); IIS- Fundación Jiménez Díaz Hospital, Madrid, Spain (B.I.); CIBER de enfermedades CardioVasculares (CIBERCV), Madrid, Spain (R.F.-J., C.G.-A., L.F.-F., C.G.-M., J.A., A.B.-G., S.R., B.I.); Cardiology Department, Hospital Universitari i Politecnic La Fe, Valencia, Spain (J.A.).

*Dr Bobi and Dr Solanes contributed equally to this study.

Correspondence to: Montserrat Rigol, DVM, PhD, Department of Cardiology, Institut Clínic de Malalties Cardiovasculars, Hospital Clínic de Barcelona, Villarroel 170, Barcelona 08036, Spain. E-mail: mrigol@clinic.cat

Received March 1, 2017; accepted March 30, 2017.

Stem cell therapy has taken on the ambitious objective of regenerating the myocardium after acute myocardial infarction (AMI). Although complete functional regeneration has not been achieved, diverse stem cell lineages have shown properties that result in important beneficial effects in the infarcted myocardium.[1–4] In this context, adipose tissue–derived mesenchymal stem cells (ATMSCs) have shown remarkable outcomes in small-animal studies,[5–7] ameliorating adverse cardiac remodeling and improving ventricular function and myocardial vascularization. These findings could be related to secretion of anti-apoptotic, pro-angiogenic, and anti-inflammatory cytokines and growth factors. Some of these therapeutic mechanisms have been described in vitro and using small-animal models,[8–10] but no experiments in large animals have evaluated the early mechanisms involved in the long-term outcomes.

Moreover, although our group has reported better benefits of ATMSCs intracoronary administration immediately after the reperfusion,[11] the ideal dosage, route, and timing for cell administration remains unresolved.[12] Furthermore, as AMI is unpredictable, allogeneic stem cells must always be immediately available when needed. Preclinical studies[13] and the POSEIDON (Percutaneous Stem Cell Injection Delivery Effects on Neomyogenesis) trial[14] have found allogeneic cell delivery to be as safe and effective as therapies using autologous sources. Nevertheless, long-term cardiac benefits of allogeneic ATMSCs therapy on reperfused hearts must be studied at length in large-animal models of AMI before the treatment can advance to the clinical phase.

Therefore, the aim of the present study was to analyze the short- and long-term effects of allogeneic ATMSCs therapy on immune response, myocardial vascularization, and cardiac function and perfusion assessed by cardiac magnetic resonance (CMR), as well as the mechanisms involved, in a translational porcine model of AMI.

Methods

The study protocol was approved by the Animal Experimentation Ethics Committee of the National Center for Cardiovascular Research (Spanish acronym, CNIC) following the Communities Council Directive 2010/63/UE and Spanish (RD 53/2013) regulations related to the Guide for the Care and Use of Laboratory Animals.

Study Design

A total of 41 Large White pigs were used in this study. Three male pigs (56.5±2.2 kg; 5–6 months old) served as adipose tissue donors and 38 female pigs (35.1±2.7 kg; 3–4 months old) underwent a reperfused AMI after 50-minute occlusion of the left anterior descending (LAD) coronary artery. Four animals died during the procedure; the 34 remaining animals were randomized into experimental (ATMSCs-treated) and control (vehicle-treated) groups stratified by follow-up: short-term follow-up (2 days post-AMI), ATMSCs (n=10) and vehicle (n=10); and long-term follow-up (60 days post-AMI), ATMSCs (n=7) and vehicle (n=7). One ATMSCs animal assigned to short-term follow-up was excluded from analysis because of incomplete reperfusion attributable to technical failure, leaving 9 animals in this group and a total of 33 animals in the analysis (Figure 1A). Protocol timelines for molecular, imaging, and histological analysis are summarized in Figure 1B.

Subcutaneous Adipose Tissue Collection and Cell Isolation, Culture, and Labeling

Subcutaneous adipose tissue from donor animals was excised from the ventral neck area and kept at 4°C in phosphate-buffered saline (Sigma-Aldrich, St. Louis, MO) supplemented with 1% penicillin/streptomycin (Gibco, Grand Island, NY). Cells were isolated and cultured as described previously.[11,15] The cells were expanded in α-minimal essential medium (Sigma-Aldrich) supplemented with 10% fetal bovine serum, 1 mmol/L L-glutamine, and 1% penicillin/streptomycin (Gibco), and 5 μg/mL Plasmocin™ (Invitrogen) under standard culture conditions (37°C, 5% CO_2), with medium replacement every 3 days. Third-passage cells were labeled by transduction (2×10^6 transducing units/mL multiplicity of infection=21, 48 hours) with a lentiviral vector containing enhanced green fluorescent protein (GFP) under constitutive transcriptional control.[16] Cells expressing GFP were selected by fluorescence-activated cell sorting and frozen before in vivo administration.

AMI Procedure and Intracoronary Administration

The same day of the intervention, animals received oral clopidogrel (150 mg/animal). Antiaggregant therapy was continued 2 days after the AMI induction (clopidogrel 75 mg/animal per day). Anesthesia was induced by an intramuscular injection of ketamine (20 mg/kg), xylazine (2 mg/kg), and midazolam (0.5 mg/kg) and maintained with continuous intravenous infusion of ketamine (2 mg/kg per hour), xylazine (0.2 mg/kg per hour), and midazolam (0.2 mg/kg per hour) and by analgesia with intravenous fentanyl (0.007 mg/kg per hour). Animals were intubated and supportive mechanical ventilation was maintained during the AMI procedure. Sheaths (6F) were percutaneously placed in the femoral artery and vein for drug administration and blood collection, and a heparin bolus of 9000 IU was given before coronary catheterization. AMI was then induced as previously described.[17–19] Briefly, the LAD was cannulated with a 5F guide catheter, by which a coaxial balloon catheter was advanced past the first diagonal branch. Once placed, the

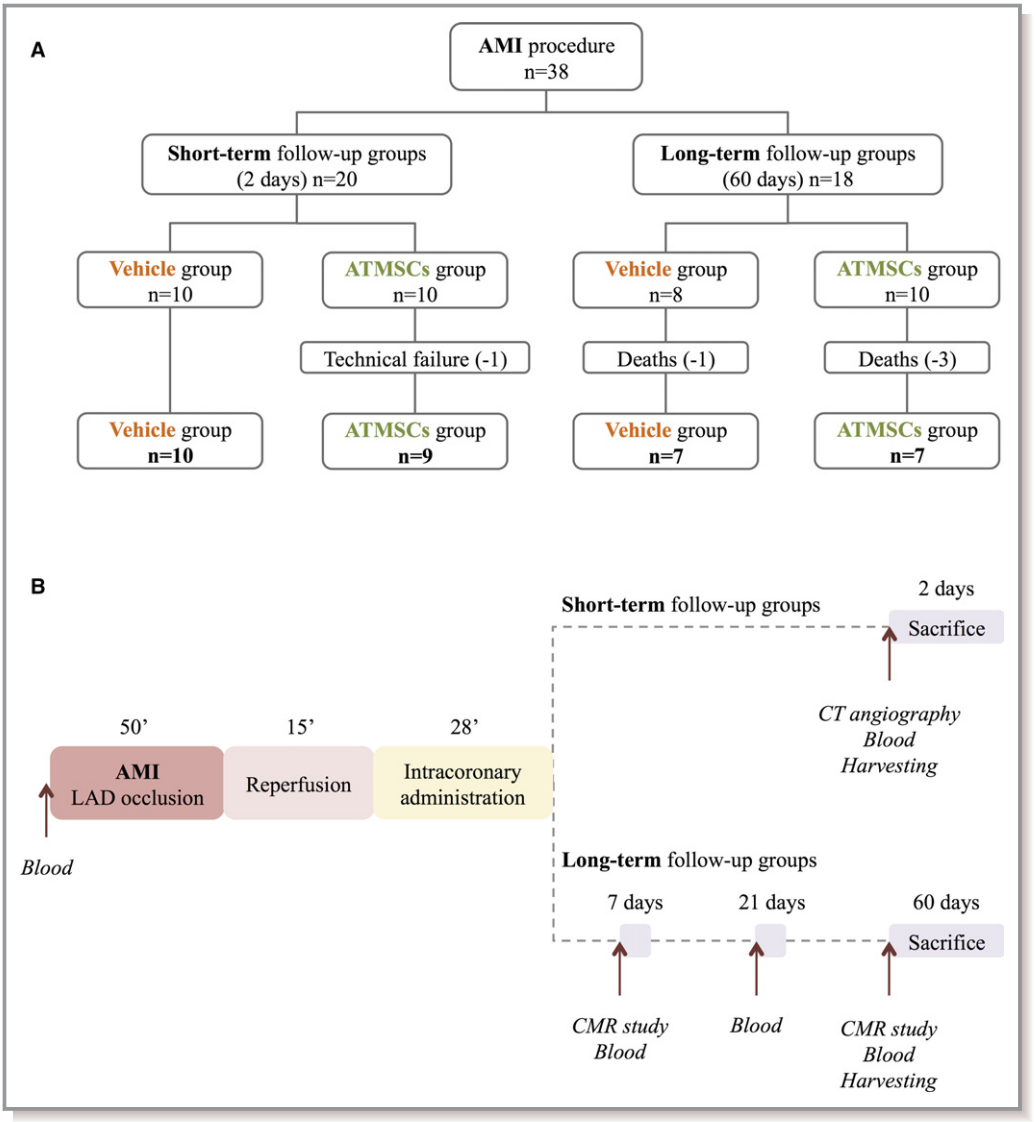

Figure 1. Flow chart illustrating the study design (A) and timeline (B). AMI indicates acute myocardial infarction; ATMSCs, adipose tissue-derived mesenchymal stem cells; CMR, cardiac magnetic resonance; CT, computed tomography; LAD, left anterior descending coronary artery.

balloon was inflated at low pressure and ischemia was maintained for 50 minutes. LAD occlusion was confirmed angiographically. During ischemia, a continuous infusion of amiodarone (5.5 mg/kg per hour) was administered to prevent malignant ventricular arrhythmias. A biphasic defibrillator was used in case of ventricular fibrillation episodes.

After 50 minutes occlusion, the balloon was deflated. Fifteen minutes after reperfusion, 10^7 ATMSCs suspended in 14 mL of Dulbecco's Modified Eagle Medium or Dulbecco's Modified Eagle Medium without cells, depending on the study group, were administered through the coaxial catheter. In order to minimize ischemia during the intracoronary delivery, 7 boluses of 2 mL (1 mL/min) Dulbecco's Modified Eagle Medium with the balloon inflated were interspersed with 2-minute periods of blood flow restoration with the balloon deflated.

Cardiac Imaging Studies

All cardiac imaging studies were performed with the animals under anesthesia. In the short-term follow-up groups, a computed tomography (CT) 64-slice scanner (Brilliance iCT; Philips Medical Systems, Best, The Netherlands) was used to evaluate LAD patency before euthanizing the animals (Figure 1B). Analysis of CT images was performed on a dedicated advanced image processing workstation (Extended Brilliance Workspace 3.5; Philips Medical Systems, Cleveland, OH) by 2 independent blinded investigators using mainly multiplanar reconstructions. In the long-term follow-up groups, CMR study was performed at 7 and 60 days (Figure 1B) with an Achieva 3T-TX whole-body scanner (Philips Healthcare, Best, The Netherlands) equipped with a 32-element phased-array

cardiac coil as previously described.[20] Each study consisted of a cine steady-state free-precision sequence to determine left-ventricular end-diastolic volume, left-ventricular end-systolic volume, and left ventricular ejection fraction[21]; late gadolinium-enhanced sequence to determine infarct size and microvascular obstruction (MVO); and (only at the 7-day CMR) a T2-weighted short-tau inversion recovery sequence to determine the extent of myocardial edema.[21] Absolute cardiac perfusion was estimated using dynamic acquisition with dual-saturation (TS=20, 80 ms) technique to avoid signal saturation during gadolinium-based contrast administration.[22] After perfusion maps generation, region-of-interest analysis was done at the infarcted core, infarct borders (anterior wall and septum), and remote myocardium.

Images were analyzed by 2 independent blinded investigators, and processed with analysis software (QMass MR 7.5; Medis, Leiden, The Netherlands and MR Extended Work Space 2.6; Philips Healthcare) as previously described.[21] In case of lack of agreement between the conclusions of the 2 investigators, the discordant images were reviewed by a third blinded investigator.

Assessment of Circulating Cytokines and Donor-Specific Antibodies

In the short-term follow-up groups, blood samples were obtained at baseline before AMI induction and at 2 days post-AMI. In the long-term follow-up groups, blood sampling was carried out at baseline and at 7, 21, and 60 days post-AMI (Figure 1B). In a randomized subset of animals (short-term follow-up groups, 7 vehicle and 8 ATMSCs-treated; long-term follow-up groups, 5 vehicle and 5 ATMSCs-treated), serum quantification of interleukin-10 (IL-10) and granulocyte-macrophage colony-stimulating factor (GM-CSF) was performed with the cytokine multiplex assay (Quantibody® Porcine Cytokine Array 1; RayBiotech, Norcross, GA). In addition, circulating levels of stromal-derived factor-1α (SDF-1α) and hepatocyte growth factor (HGF) were assessed in 5 animals from each of the 4 groups using pig SDF-1α and HGF ELISA kits, respectively (Cusabio Biotech, Wuhan, China). All protocols were performed according to manufacturer instructions. To analyze antibody-mediated rejection, crossmatch tests were performed on serum samples from ATMSCs-treated animals in the long-term follow-up group at 21 and 60 days, as previously described.[11]

Tissue Harvesting

At 2 (short-term follow-up groups) or 60 days (long-term follow-up groups), animals were euthanized and hearts were harvested (Figure 1B). Hearts were cut into transversal slices and representative sections were obtained from the anterior core infarcted wall, septum and anterior border zones, and remote posterior wall of the left ventricle. Tissue samples were fixed with 4% formaldehyde and embedded in paraffin for histological studies as previously reported.[15] Tissue samples for molecular biology studies were maintained in Allprotect Tissue Reagent (Qiagen, Hilden, Germany) until storage at −80°C. Samples were also collected from lung, thoracic lymphatic nodes, liver, jejunum, spleen, and kidney for histological and molecular analysis to track delivered GFP-ATMSCs.

Histology

Histological analysis was performed on 4-μm sections of paraffin-embedded specimens. ATMSCs retention in the infarcted myocardium and border zones was determined by immunofluorescence, using chicken anti-GFP (1:1000, ab13970; Abcam, Cambridge, MA) and cardiac troponin I (1:200, sc-15368, Santa Cruz Biotechnology, Santa Cruz, CA) as primary antibodies.

Apoptotic cells in the infarcted tissue and border zones were stained with terminal deoxynucleotidyl transferase TdT-mediated dUTP nick-end-labeling technique using the In Situ Cell Death Detection Kit, Fluorescein (Roche Applied Science, Indianapolis, IN) according to manufacturer instructions. Vascular density was assessed by double immunohistochemistry with anti-vonWillebrand factor (1:200, A0082; Dako, Carpinteria, CA) and anti-smooth muscle actin (1:100, M085101; Dako) antibodies.[11] Small vessels (<15-μm diameter) were counted in the border zones. Inflammatory cellular infiltration was studied in the infarct and border zones by detection of lymphocytes T with anti-CD3 (1:100, M0701; Dako),[11] total macrophages with CD107a (1:100, MCA2315GA; Bio-Rad, Kidlington, UK), and the M2-polarized subgroup with CD163 (1:100, bs2527R; Bioss, Beijing, China) antibodies. Collagen deposition in the remote area and the infarct zone was determined by picrosirius red staining. Stained samples from the infarct zone were also analyzed with circularly polarized light to determine collagen I and III.

All histological analyses were performed by 2 independent blinded investigators.

Quantitative Real-Time Polymerase Chain Reaction

mRNA expression of GFP, IL-10, HGF, GM-CSF, SDF-1α, vascular endothelial growth factor (VEGF), hepatocyte growth factor receptor, extracellular signal–regulated kinase 1, and secreted frizzled-related protein 2 were determined in the central infarct zone by quantitative real-time polymerase chain reaction (qPCR), based on SYBR® Green fluorescence as previously described.[23] qPCR was performed using the ViiA™

Table 1. Primer Sequences for Quantitative RT-PCR

Gene	Oligo Name	Oligo Sequence (5′ to 3′)
CSF2 (*NM_214118.2*)	GM-CSF Forward	GGATTGCTCCCACTGACAGA
	GM-CSF Reverse	GCAAGTCTGTGCCCCATTAC
IL-10 (*NM_214041.1*)	IL10 Forward	GGGAAACCCTGCTGTACCTC
	IL10 Reverse	TGAACACCATAGGGCACACC
SDF-1α (*NM_001009580.1*)	SDF-1α Forward	CCGAACTGTGCCCTTCAGAT
	SDF-1α Reverse	ATAAACATCCCGCCGTCCTC
HGF (*XM_013979787.1*)	HGF Forward	TGCTCCTCCCTTCCCTACTC
	HGF Reverse	CCCGATAGCTCGAAGGCAAA
VEGF (*AF318502.1*)	VEGF Forward	CCACGAAGTGGTGAAGTTCATG
	VEGF Reverse	CCACCAGGGTCTCGATTGG
MET (*NM_001038008*)	HGFR Forward	CAGAAGAGCAAGGGAGAGTGT
	HGFR Reverse	GGGCACCCAGGTAAATGTGAT
MAPK3 (*XM_013991188.1*)	ERK-1 Forward	GGCTCATCCTTACCTGGAGC
	ERK-1 Reverse	AGATGAGTTCCTTCAGCCGC
SFRP2 (*NM_001244395.1*)	SFRP-2 Forward	CCCGACTTCTCCTACAAGCG
	SFRP-2 Reverse	GCCGCATGTTCTGGTACTCT
ACTB (*XM_003124280.4*)	β-Actin Forward	GTGACAGCAGTCGGTTGGAT
	β-Actin Reverse	TTTTGGGAAGGCAGGGACTT

ACTB indicates actin beta; CSF, colony-stimulating factor; HGF, hepatocyte growth factor; GM-CSF, granulocyte-macrophage colony-stimulating factor; IL-10, interleukin-10; MAPK3, mitogen-activated protein kinase 3; MET, MET proto-oncogene; RT-PCR, reverse transcription polymerase chain reaction; SDF-1α, stromal-derived factor-1α; SFRP2, secreted frizzled-related protein 2.

7 Real-Time PCR System (Applied Biosystems, Foster City, CA). Primer sequences used are described in Table 1.

Real-Time PCR for GFP mRNA Quantification

The GFP mRNA in infarcted myocardium and border zones was quantified using SYBR® Green–based real-time PCR protocol. Reverse-transcribed GFP cDNA was amplified, starting with 100 ng of total cDNA and using the primer pair 5′-AAGTTCATCTGCACCACCG′-3′ (GFP-Forward) and 5′-TCCTTGAAGAAGATGGTGCG-3′ (GFP-Reverse). Number of GFP transcript copies was established by comparison to a calibration curve based on known amounts of GFP DNA from GFP expression control vector (pLenti6.2-GW/EmGFP; Invitrogen, Waltham, MA). The standard curve for GFP DNA was obtained by 10-fold serial dilution from 1 ng (3×10^6 copy number of GFP) to 1 fg (3 copy number of GFP) of the GFP expression control vector (Figure 2). A concomitant quantification of β-Actin mRNA (input and reverse transcription control) was performed for each experimental sample.

Statistical Analysis

SPSS software (IBM SPSS Statistics for Windows, Version 23.0, released 2013; IBM Corp, Armonk, NY) was used to perform statistical analysis and GraphPad Prism (version 5.00 for Windows; GraphPad Software, San Diego, CA) to create the graphics dots. Normal distribution was assessed with the Kolmogorov–Smirnov test and confirmed by visually checking the distribution of the variables. Continuous normal distributed variables were studied with the *t* test and are represented as mean±SD; non-Gaussian continuous variables were assessed by Mann–Whitney test and represented as median and [interquartile range] (25th–75th percentiles). Qualitative variables (mortality) were compared using the Fisher exact test. Time-dependent comparisons of CMR-derived myocardial perfusion obtained at day 7 and day 60 within each group were studied with paired *t* test. Linear regression of standard curve obtained from serial dilutions of the pLenti6.2-GW/EmGFP plasmid was used to calculate GFP mRNA quantification by real-time PCR.

Results

AMI Procedure and Mortality

At 2 days post-AMI, LAD angiography revealed occlusion, induced by a technical failure, in only 1 of the 20 animals assessed by CT. This animal was excluded from analyses. During the first 48 hours after AMI induction, 4 animals died

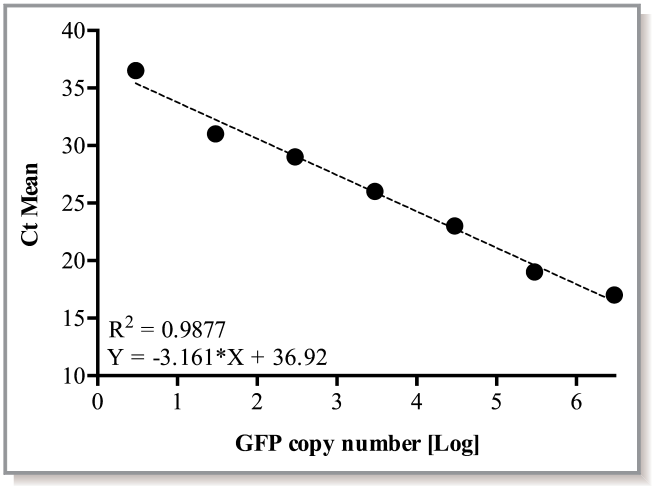

Figure 2. Linear regression of standard curve obtained from serial dilutions of the pLenti6.2-GW/EmGFP plasmid (3—3×10^6 copy number) assayed in duplicate by qPCR. R^2 and equation of linear regression are described in the intersection point of the chart. Ct indicates threshold cycle; GFP, green fluorescent protein; qPCR, quantitative real-time polymerase chain reaction.

(10.5%, without significant differences between study groups) (Figure 1A). One animal (ATMSCs group) died during AMI induction because of malignant arrhythmia. Three more animals (1 from control group, 2 from ATMSCs group) died post-AMI in the animal facilities, presumably because of malignant arrhythmia related to AMI.

Effectiveness and Safety of Cell Delivery

Myocardial ATMSCs engraftment after intracoronary administration was evaluated by GFP tissue detection in the short-term (2 days) and long-term (60 days) groups. Immunohistochemical analysis showed 4±3 GFP-positive cells per histological section both in the infarcted myocardium and border zone at 2 days post-AMI (Figure 3). GFP expression was also detected by qPCR in the infarcted tissue (21.17±12.0 copies of GFP) and more markedly in the border zone (96.07±35.7 copies of GFP). Moreover, 30.9% of the observed GFP-positive cells were terminal deoxynucleotidyl transferase TdT-mediated dUTP nick-end-labeling–positive. In the long-term groups, we found no GFP-positive cells in the histological study and detected no GFP gene signal by qPCR. No sign of engrafted GFP-positive cells was detected in remote organs in any group.

Inflammatory infiltration was evaluated by histological analysis at 2 days in the short-term groups and at 60 days in the long-term groups. Table 2 shows the number of lymphocytes T and macrophages found in the infarcted myocardium and at the border zone. No significant differences were observed between groups. However, at 60 days, an elevated number of T lymphocytes was observed in 2 animals (483.6 and 1085.5 CD3-positive cells/mm^2) receiving ATMSCs, and 1 of them was also crossmatch test positive for humoral immunity. No donor-specific antibodies in serum were found in the other 6 animals receiving allogeneic ATMSCs at 60 days post-AMI.

No coronary artery vasospasm was detected while administering the ATMSCs. MVO was assessed by CMR in the long-term follow-up groups at 7 days post-AMI as safety end point. No significant differences were observed between vehicle animals and those receiving ATMSCs (6.0±8.1% versus 6.2±7.2% of infarct, respectively; P=0.960).

Vascular Density

Vascular density was similar in both short-term follow-up groups (49.1±9.1 in vehicle versus 57.1±15.1 <15-μm vessels/mm^2 in ATMSCs; P=0.176). In contrast, in the long-term follow-up groups, a significant increase in small vessels was detected in the infarct border zones of animals treated with ATMSCs, compared with vehicle-treated (118±18 versus 92.4±24.3 <15-μm vessels/mm^2, respectively; P=0.045) (Figure 4A).

Cardiac Function, Edema, Infarct Tissue, and Perfusion by CMR Imaging

CMR values from the long-term follow-up groups are summarized in Table 3. At 7 days, no statistical differences were observed between vehicle and ATMSCs groups in the infarct size normalized by edema extent, as determined by CMR (0.96±0.04 versus 0.95±0.06, respectively; P=1.000). At 60-day follow-up, scar size was also similar between vehicle and ATMSCs-treated animals (19.1±4.3% versus 15.4±4.7% of left ventricle, respectively; P=0.153) (Figure 5).

Left ventricle functionality study showed no significant differences between groups at 7 or at 60 days in terms of left-ventricular end-diastolic volume, left ventricular end-systolic volume, or left-ventricular ejection fraction. Myocardial perfusion of the anterior infarct border was significantly higher 7 days after the intervention in the animals treated with ATMSCs, compared with the vehicle group (87.9±28.7 versus 57.4±17.7 mL/min per gram, respectively; P=0.034). This difference was remarkably higher at 60 days post-AMI (99±22.6 versus 43.3±14.7 mL/min per gram; P=0.0001) (Figure 4B).

Mechanisms Involved in ATMSCs Effects

Pro-angiogenic factors

The studies of pro-angiogenic mechanisms revealed a higher expression of SDF-1α and GM-CSF genes in the infarcted tissue of ATMSCs-treated animals, compared with

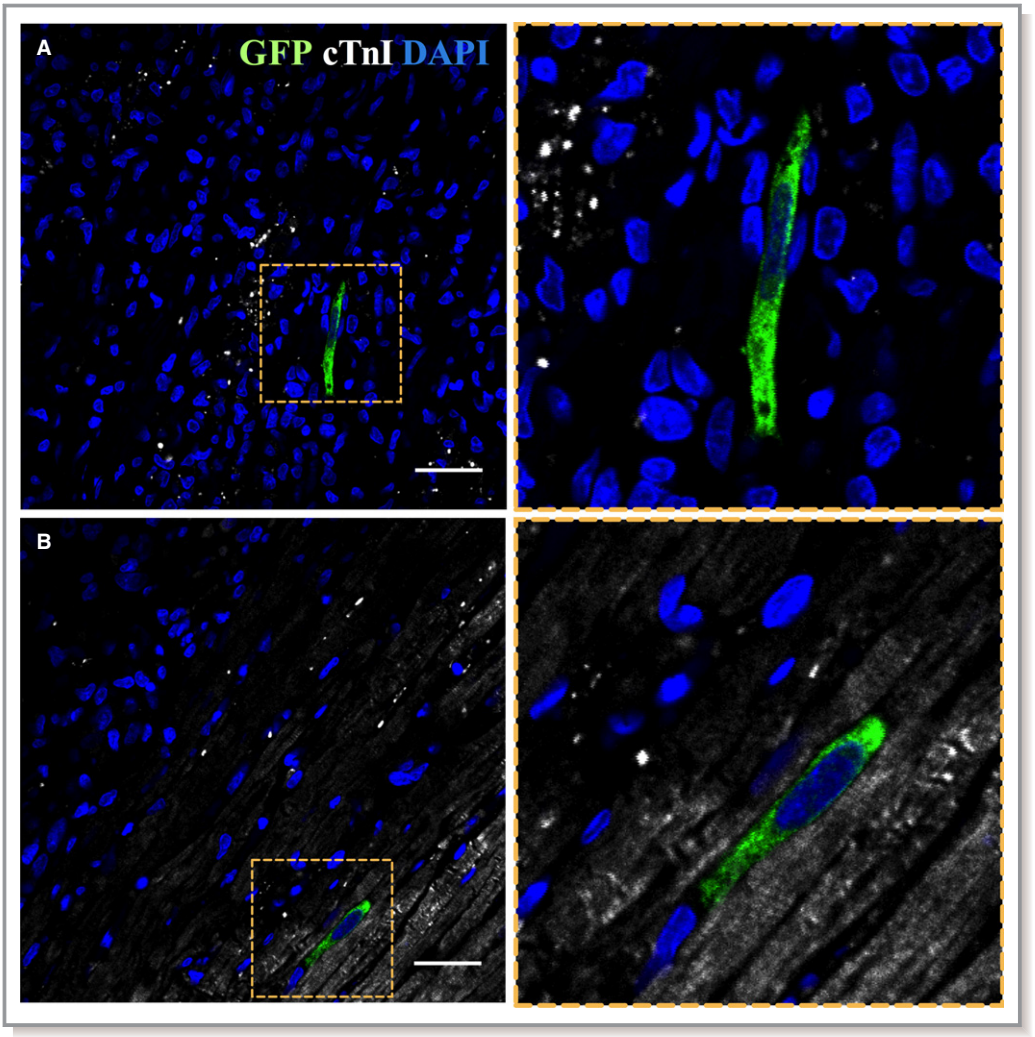

Figure 3. ATMSCs implantation in the myocardium. Confocal microscopy images showing GFP-positive ATMSCs (green) in the infarct area (A) and border zone (B) (cTnI in white and nuclei counterstained with DAPI in blue). Right panels represent zoom images from the left panels. Scale bars, 50 μm. ATMSCs indicates adipose tissue-derived mesenchymal stem cells; cTnI, cardiac troponin-I; DAPI, 4′,6-diamidino-2-phenylindole dihydrochloride; GFP, green fluorescent protein.

vehicle-treated, at 2 days. VEGF was also augmented in the infarct zone in the ATMSCs group (Figure 4C). Nevertheless, at 60 days, no significant differences in SDF-1α, VEGF, and GM-CSF genes expression were observed among groups.

Analysis of circulating pro-angiogenic factors in the serum showed a significant increase in GM-CSF at 2 days post-AMI in animals treated with ATMSCs, compared with vehicle (1.69±1.08 versus 0.05±0.62 log2 fold change, respectively; *P*=0.003). However, decreased GM-CSF was detected in serum of ATMSCs-treated animals, compared with vehicle-treated, at 7 (−0.32±0.32 versus 0.35±0.15 log2 fold change, respectively; *P*=0.003) and 60 days (−0.93±0.81 versus 1.15±0.93 log2 fold change, respectively; *P*=0.006).

Table 2. CD3-Positive Cells (Lymphocytes T) and CD107a-Positive Cells (Macrophages) per mm^2 of Myocardium

	Short-Term Follow-Up			Long-Term Follow-Up		
	Vehicle (n=10)	ATMSCs (n=9)	*P* Value	Vehicle (n=7)	ATMSCs (n=7)	*P* Value
T lymphocytes	202.6±90	206.4±61.5	0.916	141.8±48.1	345.9±352.6	0.155
Macrophages	1383.7±407.6	1451.8±401	0.718	42.7±18.8	59.8±20.2	0.126

Values are represented as mean±SD. ATMSCs indicates adipose tissue-derived mesenchymal stem cells.

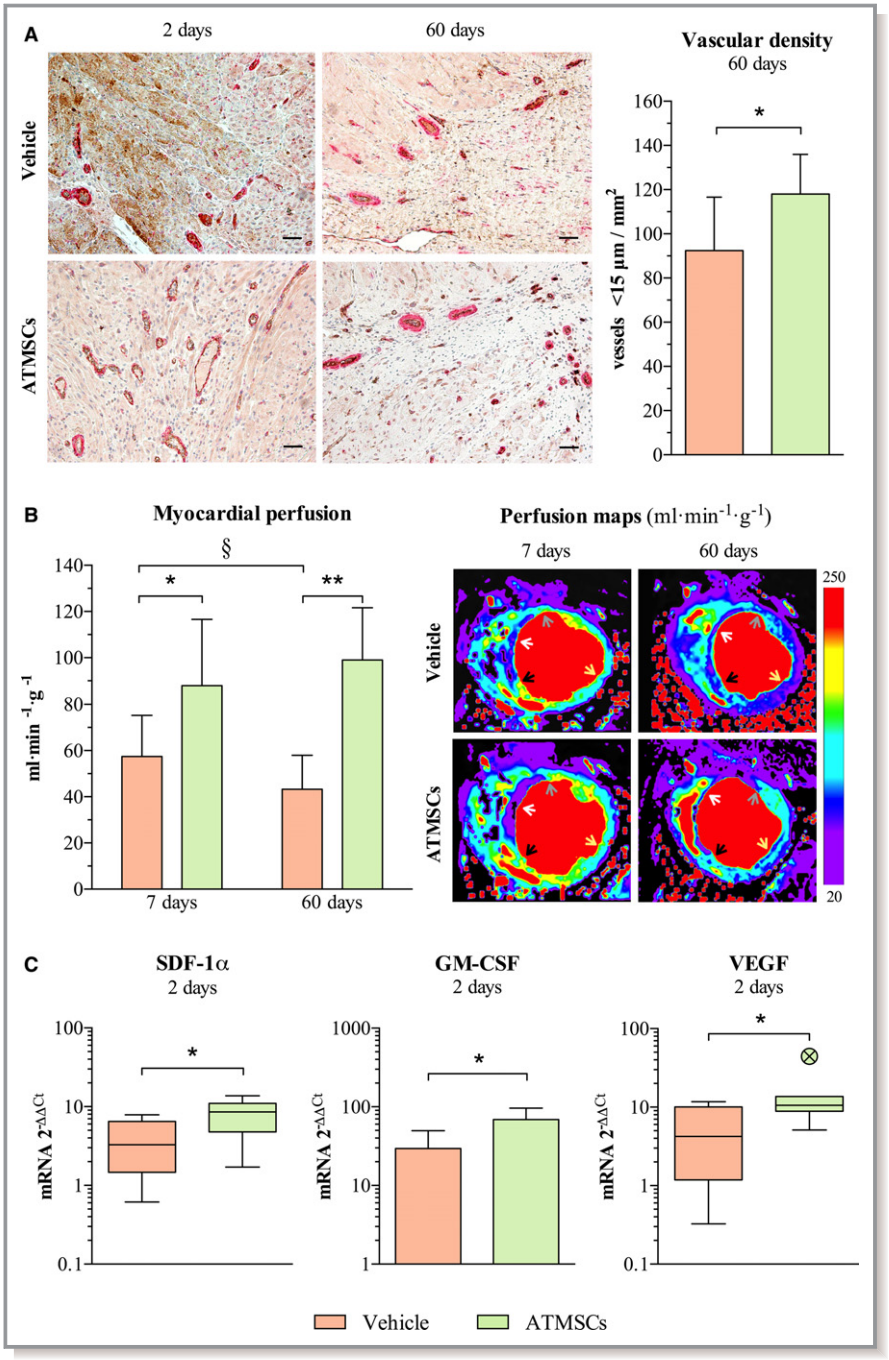

Figure 4. Effects of ATMSCs therapy on myocardial vascularization and perfusion. A, Microphotographs on the left (endothelial cells stained in brown and smooth muscle cells stained in red) and bar chart on the right showing increased vessel density in the border infarct zone of animals receiving cell therapy. B, Bar chart on the left and cardiac magnetic resonance images (myocardial quantitative perfusion maps) on the right illustrate an enhancement on myocardial perfusion of infarct border zone in animals receiving allogeneic ATMSCs. Arrows point to perfusion analysis region of interest (gray, anterior infarct border; white, core infarcted area; black, septum infarct border; yellow, posterior remote myocardium). C, Charts show up-regulation of the pro-angiogenic mediators SDF-1α, GM-CSF, and VEGF in the infarcted tissue of the ATMSCs group compared with vehicle group, as assessed by qPCR. **P*<0.05 between groups; ***P*<0.01 between groups; §*P*<0.05 paired *t* test. Scale bars, 50 µm. ATMSCs indicates adipose tissue-derived mesenchymal stem cells; GM-CSF, granulocyte-macrophage colony-stimulating factor; qPCR, quantitative real-time polymerase chain reaction; SDF-1α, stromal-derived factor 1α; VEGF, vascular endothelial growth factor.

Table 3. CMR Results

	7 Days Post-AMI			60 Days Post-AMI		
	Vehicle (n=7)	ATMSCs (n=7)	*P* Value	Vehicle (n=7)	ATMSCs (n=7)	*P* Value
LVEDV, mL	133.2±17.0	133.4±22.6	0.986	201.3±37.3	190. 6±37.2	0.600
LVESV, mL	80.3±16.9	74.3±15.9	0.510	126.5±35.8	110.6±30.4	0.387
LVEF, %	40.2±5.2	44.4±3.6	0.110	37.9±6.3	42.7±5.2	0.142
Infarct size (% LV)	30.8±5.5	25.0±5.0	0.061	19.1±4.3	15.4±4.7	0.153
MVO (% infarct)	6.2±7.2	6.0±8.1	0.960	—	—	—
Edema (% LV)	32.1±5.4	26.3±4.9	0.059	—	—	—
Infarct size (% edema)	0.96±0.04	0.95±0.06	1.000	—	—	—
Myocardial perfusion, mL/min per gram						
Core infarcted area	52.7±35.0	45.6±22.9	0.658	64.5±16.7	69.8±19.6	0.618
Anterior infarct border	57.4±17.7	87.9±28.7	0.034	43.3±14.7	99.0±22.6	<0.001
Septum infarct border	65.5±26.6	71.9±14.8	0.588	60.6±3.7	76.2±30.1	0.237
Posterior remote wall	214.3±73.3	212.5±76.8	0.965	120.2±3.7	179.3±87.5	0.118

Values are represented as mean±SD. Edema sequences and MVO were only available at the 7-day CMR study.[18] AMI indicates acute myocardial infarction; ATMSCs, adipose tissue-derived mesenchymal stem cells; CMR, cardiac magnetic resonance imaging; LV, left ventricle; LVEDV, left ventricular end-diastolic volume; LVEF, left ventricular ejection fraction; LVESV, left ventricular end-systolic volume; MVO, microvascular obstruction.

Dynamics of circulating SDF-1α were similar between groups at short- and long-term follow-up (Figure 6).

Anti-apoptotic effects

The percentage of apoptotic cells in the infarct zone was significantly lower in the ATMSCs-treated animals compared with vehicle at 2 days post-AMI (48.6±6% versus 55.9±5.7%, respectively; *P*=0.017). No differences between groups were observed in the border zone (Figure 7A). Study of anti-apoptotic pathways showed a significant increase in circulating HGF levels in the ATMSCs group (Figure 7B). Moreover, hepatocyte growth factor receptor, extracellular signal–regulated kinase 1, and secreted frizzled-related protein 2 genes were up-regulated in the infarcted myocardium of ATMSCs-treated animals (Figure 7C). At 60 days, there were no differences in hepatocyte growth factor receptor, extracellular signal–regulated kinase 1, and secreted frizzled-related protein 2 genes expression between vehicle and ATMSCs groups. HGF gene expression was similar at 2 and 60 days post-AMI in the infarcted tissue of both vehicle and ATMSCs-treated animals. The long-term follow-up groups were also similar in their circulating HGF dynamic (Figure 7B).

Anti-inflammatory mechanisms

The analysis of possible anti-inflammatory mechanisms at 2 days post-AMI showed a significantly higher percentage of alternatively activated M2 (CD163-positive) macrophages with respect to total number of (CD107a-positive) macrophages in the infarct zone of ATMSCs-treated animals, compared with vehicle-treated (67.2±10% versus 54.7±10.2%, respectively; *P*=0.016) (Figure 8A). A higher expression of IL-10 gene was observed in the infarcted tissue of ATMSCs animals, compared with vehicle, in the short-term follow-up groups. Moreover, this anti-inflammatory cytokine (IL-10) was increased at 2 days in systemic blood of animals treated with ATMSCs (Figure 8B). In the long-term follow-up groups, a significant increase in the circulating IL-10 was found in the ATMSCs group only at 60-day follow-up (0.99±2.67 versus vehicle, −3.64±3 log2 fold change, respectively; *P*=0.032). Nevertheless, no significant differences were observed in the expression of IL-10 gene in the infarcted tissue (Figure 8C).

Effect on collagen deposition

Histological assessment of left ventricle remodeling at 60 days showed no differences in collagen deposition in the remote zone between vehicle and ATMSCs groups (6.3±1% versus 6.6±0.6% of area, respectively; *P*=0.525) or at the scar (38.8±10.6% versus 41.7±8.7% of area, respectively; *P*=0.597). Nevertheless, the collagen type I/type III ratio of the scar was significantly higher in ATMSCs-treated animals, compared with vehicle (1.5±0.2% versus 2.4±0.7% of area, respectively; *P*=0.010) (Figure 9).

Discussion

The present study analyzed the long-term outcomes and potential mechanisms of allogeneic ATMSCs therapy in a translational porcine model of reperfused AMI. The main

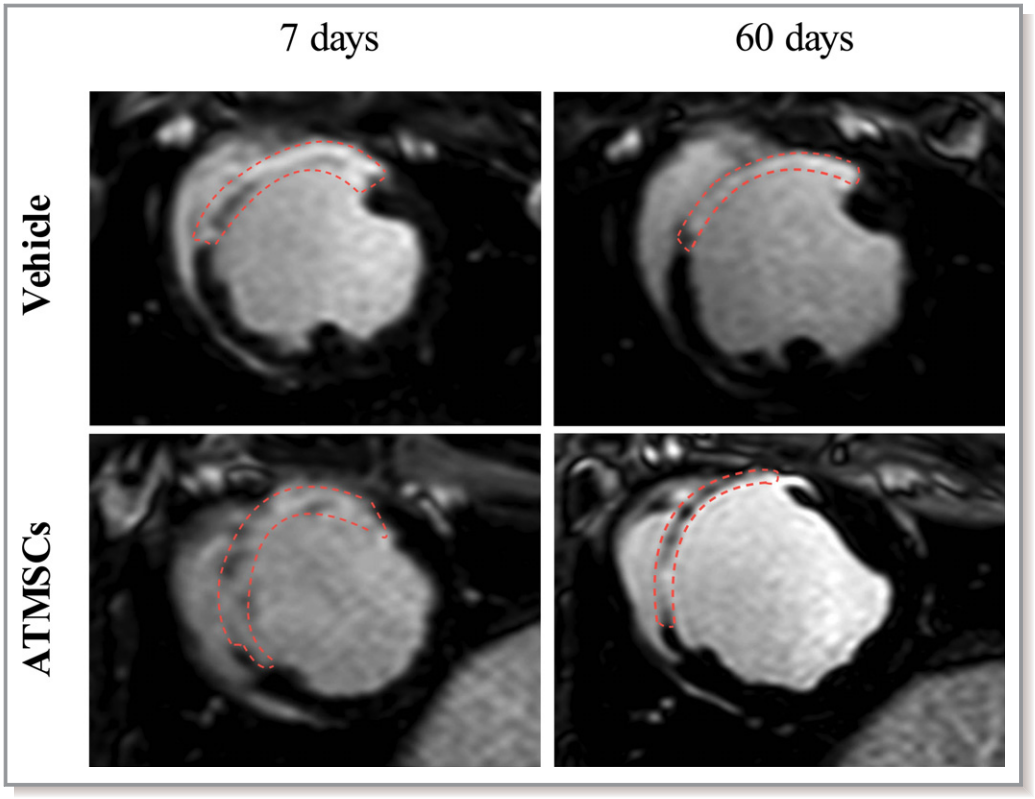

Figure 5. Late gadolinium-enhanced CMR images. Follow-up CMR analysis showed similar infarct size between controls and ATMSCs-treated animals at 7 and 60 days. Red dashed lines depict late gadolinium-enhanced infarcted myocardium. ATMSCs indicates adipose tissue-derived mesenchymal stem cells; CMR, cardiac magnetic resonance.

finding of our work was that allogeneic ATMSCs administration promoted an increase in myocardial perfusion in the ischemic tissue of animals with AMI. Moreover, a decrease in the apoptotic process and an up-regulation of anti-inflammatory and reparative mechanisms have been identified in the short-term after ATMSCs administration.

Intracoronary Delivery of Allogeneic ATMSCs

Intracoronary administration is one of the least invasive delivery methods, although infusion of large-size adult mesenchymal stem cells (MSCs) (up to 20 μm in diameter) could potentially obstruct capillaries (from 6 to 10 μm in diameter), leading to permanent no-reflow phenomena after cell administration. In this sense, clinical[24] and preclinical[25–29] studies have found that intracoronary injection of a significant number (up to 50 million) of large-size stem cells (≈20–50 μm in diameter) can be safe when administered a few days after AMI. However, microvascular injury is higher during the first 24 hours post-AMI, and therefore the probability of capillary plugging and MVO increases when administering large cells directly into the culprit artery. Although MVO persists at least 1 week after reperfusion,[30] our study found no MVO increase at 7 days post-AMI in those animals receiving 10^7 ATMSCs (≈13 μm in diameter) in the LAD just after reperfusion. Our finding agrees with most of the previous literature[11,27,31] and supports the feasibility and safety of intracoronary administration of large-size cells just after reperfusion as long as precautions are taken in determining the infusion rate and dose.

The protocol of cell administration just after reperfusion requires rapid availability of ATMSCs; the cells must be stored to use when needed and, consequently, allogeneic origin is required. An important advantage of administering allogeneic stem cells is that they could be obtained from healthy young donors, since quantitative and qualitative stem cell deterioration has been demonstrated in aged patients[32] with atherosclerotic risk factors.[33]

Host Response

Originally, MSCs were described as possessing an immunoprivileged status and immunosuppressive properties,[34] which could present an advantage for allogeneic cell therapies. In our porcine model, no significant differences between groups were observed in immune cells infiltration after cell therapy; however, 2 animals receiving allogeneic ATMSCs had increased T-lymphocyte infiltration at 60 days, which could

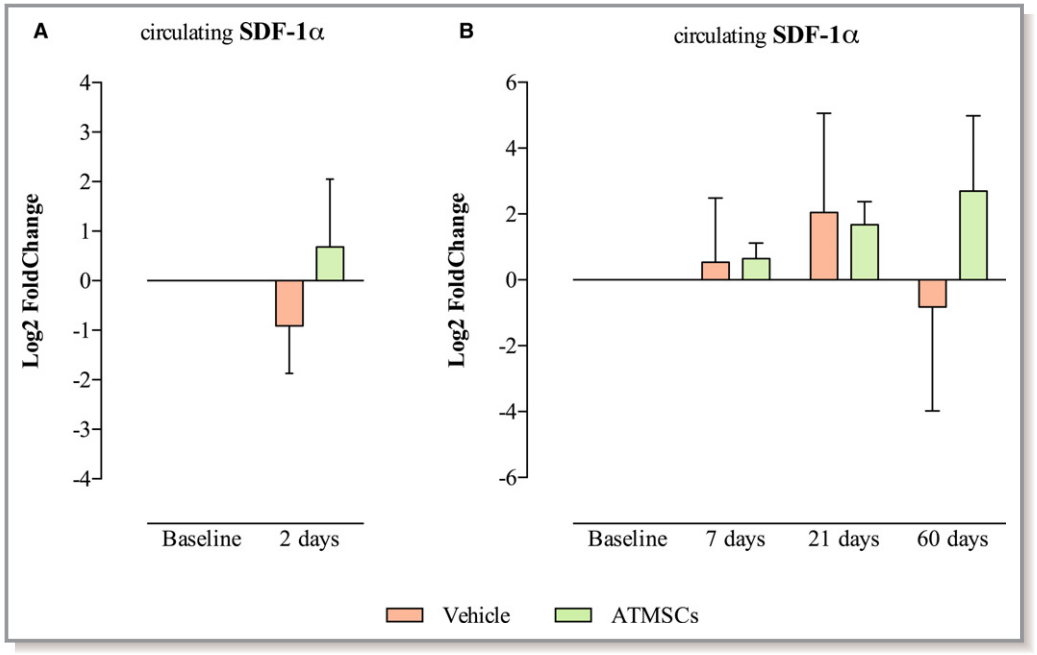

Figure 6. Bar charts represent SDF-1α in serum in the short-term follow-up (A) and long-term follow-up (B) groups. ATMSCs indicates adipose tissue-derived mesenchymal stem cells; SDF-1α, stromal-derived factor 1α.

reflect interindividual variations in the response. Moreover, only 1 of the 7 animals receiving allogeneic ATMSCs produced allo-antibodies, which agrees with the host response observed in our previous study in the same animal model[11] and a previously reported clinical trial[14] using allogeneic MSCs. Conversely, Kanazawa[35] reported the absence of humoral rejection after in vivo administration of allogeneic cardiosphere-derived cells, which could be explained by differences in source-dependent characteristics described by Ock et al.[36]

Insights Into ATMSCs Modulation of Endogenous Reparative Process and Inflammatory Response

Two days after administration, one third of implanted ATMSCs were already in apoptosis and no signal of ATMSCs presence was detected in the infarcted tissue at long-term follow-up. Nevertheless, major benefits after ATMSCs therapy were observed at 60 days, suggesting that the long-term benefits observed in our study are a consequence of changes promoted by ATMSCs in the acute phase after their administration. To test this hypothesis, we evaluated some of the mechanisms involved in the repair process and stimulation of endogenous stem cell population. In particular, we found an increase in the chemotactic mediators SDF-1α and GM-CSF at 2 days after cell administration. As previously proposed,[11,37] we would further hypothesize that endogenous stem cell stimulation could increase and continue to support the regenerative mechanisms promoted by MSC therapy, even when these cells were not present in the infarcted tissue. Accordingly, ATMSCs administration could be described as a booster therapy for the endogenous reparative process. In addition, a qualitative modification to the percentage of anti-inflammatory and pro-repair M2 macrophages was detected in our porcine model of AMI. A relationship between ATMSCs and polarization of M2 macrophages has been previously described in vitro[38] and in a porcine model of renal artery stenosis.[39] Our finding was also accompanied by a clear increase in circulating IL-10 and its mRNA in the infarcted tissue in the short term after ATMSCs administration. One of the most important anti-inflammatory mediators, IL-10 is involved in the pro-inflammatory/anti-inflammatory macrophages switch and, therefore, in setting up the reparative phase.[40]

ATMSCs Administration as a Pro-Vascularization Therapy

Improved vascular density[15,31,41] and myocardial perfusion[27,31] have been reported after autologous ATMSCs therapy. In our study, similar outcomes were found but after intracoronary administration of ATMSCs from allogeneic origin. Moreover, we identified an enhancement of 4 mediators (VEGF, HGF, GM-CSF, and SDF-1α) and M2 macrophages involved in neovascularization in the acute phase after cell administration as potential mechanisms in the improvement of myocardial perfusion. Our data suggest that these up-regulated pro-angiogenic mechanisms just 2 days after therapy could have an important role in the increase of

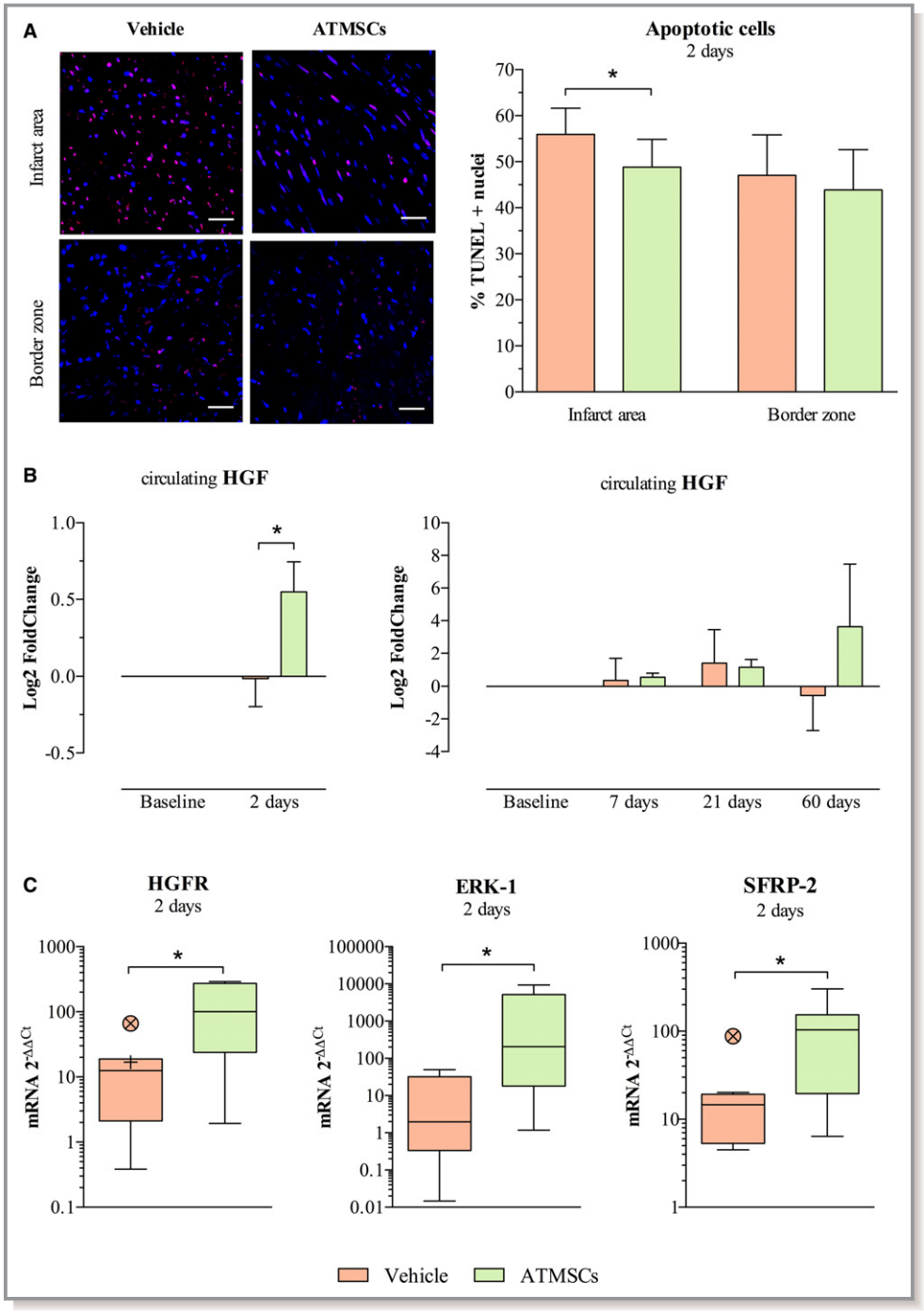

Figure 7. Analysis of apoptotic process. A, On the left, images from immunofluorescent staining (TUNEL-positive nuclei stained in magenta and total nuclei counterstained with DAPI in blue) and on the right, bar chart comparing study groups' percentage of apoptotic cells in the infarcted tissue and border infarct zone at 2 days post-AMI. B, Bar chart on the left showing an increase in the anti-apoptotic mediator HGF in serum of ATMSCs-treated animals, as measured by ELISA technique. Bar charts on the right show similar dynamics of HGF in the long-term follow-up groups. C, Box plots represent gene expression by qPCR of HGFR and ERK-1, mediators of HGF signaling pathway, and the anti-apoptotic SFRP-2 up-regulation in infarcted tissue of ATMSCs group animals. **P*<0.05 between groups. Scale bars, 50 μm. ATMSCs indicates adipose tissue-derived mesenchymal stem cells; AMI, acute myocardial infarction; DAPI, 4′,6-diamidino-2-phenylindole dihydrochloride; ERK-1, extracellular signal–regulated kinase 1; HGF, hepatocyte growth factor; HGFR, hepatocyte growth factor receptor; qPCR, quantitative real-time polymerase chain reaction; SFRP-2, secreted frizzled-related protein 2; TUNEL, terminal deoxynucleotidyl transferase (TdT)-mediated dUTP nick-end-labeling.

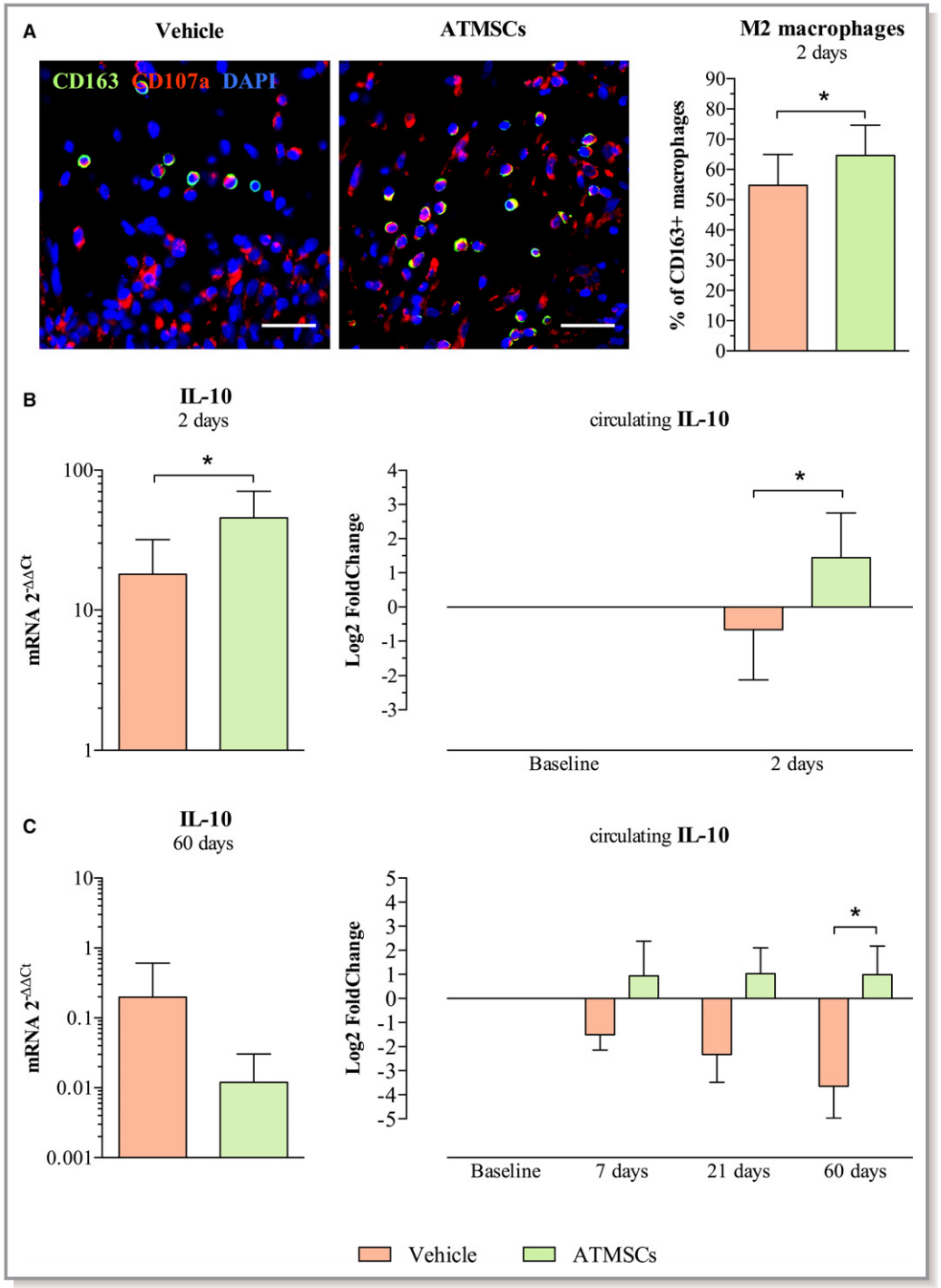

Figure 8. ATMSCs modulatory properties on inflammatory response. A, Microphotographs on the left show macrophages (CD107a-positive cells in red) and the M2 macrophages subset (CD163-positive and CD107a-positive cells, double stained in green and red) in the infarct zone. Bar chart, on the right, shows higher percentage of M2 macrophages with respect to total macrophages in ATMSCs group compared with vehicle. B, Anti-inflammatory IL-10 was found up-regulated in the infarcted tissue by qPCR (bar chart on the left) and increased in serum by ELISA (bar chart on the right) in animals receiving ATMSCs, compared with vehicle-treated at 2 days post-AMI. C, Bar chart on the left shows IL-10 gene expression assessed by qPCR in the long-term follow-up groups. The study of circulating IL-10 showed similar dynamics at 7- and 21-day follow-up in both study groups; however, a significant increase of IL-10 in serum was detected at 60 days post-AMI in ATMSCs-treated animals compared with controls (bar charts on the right). **P*<0.05 between groups. Scale bars, 20 μm. ATMSCs indicates adipose tissue-derived mesenchymal stem cells; DAPI, 4′,6-diamidino-2-phenylindole dihydrochloride; IL-10, interleukin-10; qPCR, quantitative real-time polymerase chain reaction.

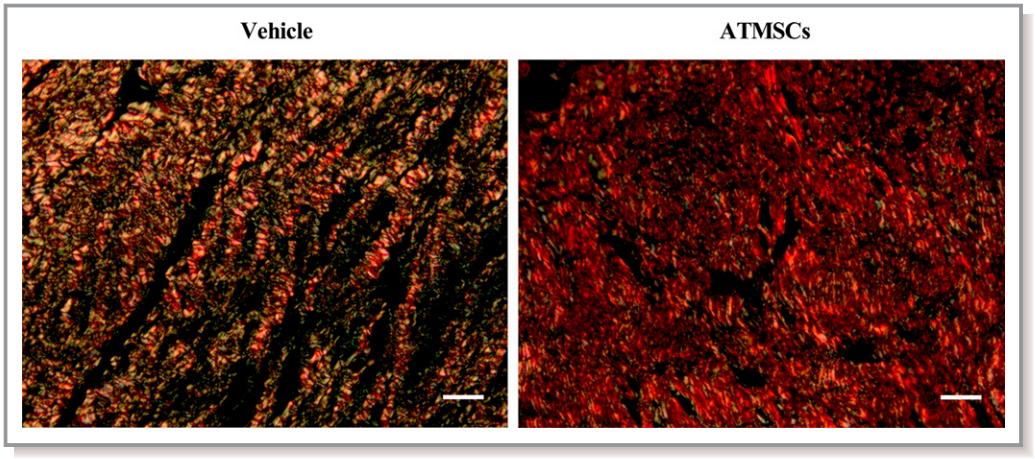

Figure 9. Images from picrosirius red staining were obtained with circularly polarized light. Collagen type I (red fibers) was more predominant in the scar from animals treated with ATMSCs than with collagen type III (green fibers). Scale bars, 50 μm. ATMSCs indicates adipose tissue-derived mesenchymal stem cells.

myocardial perfusion observed at 7-day follow-up. Given the observed trend toward better myocardial perfusion at 60 days, compared to 7 days, we hypothesize that the increase in the pro-angiogenic mediators promoted by ATMSCs therapy not only enhances the initial physiological vessel sprout but also contributes to maintain this newly established microvasculature. In contrast, we observed a significant decrease in myocardial perfusion at 60-day follow-up in the vehicle group, suggesting a certain loss of the new microvasculature established in the acute post-AMI phase. In this sense, the decrease in the apoptotic process observed after 2 days and propitiated by the ATMSCs therapy could also have an important role in promoting vessel persistence in ATMSCs-treated animals, enhancing vessel density and myocardial perfusion in the longer term.

Our main findings about myocardial vascularization and perfusion could have clinical implications for improving the patient's quality of life, as in the PROGENITOR trial.[3] The earlier clinical study showed an enhancement in myocardial perfusion together with a decrease in the number of angina episodes and improved angina functional class in patients who had refractory angina and who received a transendocardial injection of CD133+ progenitor cells.

Cardiac Function and Remodeling

Despite the lack of any reduction in infarct size or improvement in left ventricular ejection fraction, a lower percentage of apoptotic cells was detected in the infarcted tissue at 2 days after intracoronary cell administration. Our data agree with published studies demonstrating the in vivo anti-apoptotic effect of ATMSCs.[42,43] Furthermore, we described an up-regulation of potential mechanisms related to this early anti-apoptotic effect: an increase in circulating HGF was detected 2 days after ATMSCs administration, as well as an up-regulation of hepatocyte growth factor receptor and extracellular signal–regulated kinase 1 in the infarcted tissue, which are mediators of the HGF signaling pathway. HGF benefits in myocardial infarction have been postulated previously,[44,45] and its secretion by ATMSCs has been described[5] and reinforced,[46] but these previous studies did not analyze the relationship between ATMSCs therapy and an increase in systemic circulation of HGF in a clinically relevant AMI model. In the animals receiving ATMSCs, we also identified an up-regulation of the secreted frizzled-related protein 2 gene, an anti-apoptotic mediator that is secreted by MSCs and exerts cardiac protection.[47] However, despite the 10% reduction in the apoptotic process observed at 2 days post-AMI, this effect was not sufficient to reduce infarct size or enhance left ventricular ejection fraction.

Although no reduction in scar size was observed by CMR, histological analysis detected a higher ratio of type I/type III collagen in the infarcted tissue at 60 days, suggesting the establishment of a more mature and stiffer scar in the animals treated with ATMSCs. In a knock-out MMP9 mouse model of myocardial infarction, Voorhees et al[48] reported that a stiffer scar presented better ventricle mechanics, suggesting that a stiffer scar could prevent ventricular dilation. Although the stiffer scar observed in the ATMSCs-treated animals in our study could suggest less susceptibility to infarcted ventricle dilation or scar rupture, more detailed studies with longer follow-up are needed to prove this hypothesis.

Limitations

In this study, we were unable to determine baseline CMR before ATMSCs treatment because of the immediacy of the intracoronary infusion protocol (15 minutes after AMI

induction). A limitation of all animal studies is that caution is needed when extrapolating experimental results to the clinic. However, the pig is considered one of the most clinically translatable large-animal models for the study of potential therapies in the context of AMI. It has a coronary artery anatomy and distribution similar to that of humans, along with a minimal pre-existing coronary collateral flow.[49] On the other hand, cell labeling-tracking and counting is limited in a large animal because it is methodologically complicated to analyze the entire organ, and thus, we performed the analysis in representative histological samples. Another limitation when using a porcine model is that sedation is required to obtain blood samples, and consequently, the blood sampling protocol was designed considering the risks of increased mortality because of repeated sedations in the nearly days after AMI induction.

Conclusions

In summary, intracoronary administration of allogeneic ATMSC is a safe procedure and promotes the stimulation of reparative pathways, as evidenced by better myocardial vascularization and perfusion in our clinically relevant model of reperfused AMI. Although the short-term mechanisms triggered by delivered ATMSCs were insufficient to modify infarct size and left ventricle function, the local and systemic changes promoted by ATMSCs therapy suggest remarkable assets for future heart regeneration strategies.

Author Contributions

Bobi: Planning and design of study experiments. Subcutaneous adipose tissue collection, infarct procedure, intracoronary administration of cells/vehicle, CMR images analysis, and histological studies. Data analysis and interpretation. Co-writer of the manuscript. Final approval of the manuscript. Solanes: Planning and design of study experiments. Subcutaneous adipose tissue collection, infarct procedure, intracoronary administration of cells/vehicle, and histological studies. Data analysis and interpretation. Co-writer of the manuscript. Final approval of the manuscript. Fernández-Jiménez: Planning and design of the in vivo experiments and the in vivo imaging tests. Infarct procedure and intracoronary administration of cells/vehicle. Made critical revision to the manuscript. Final approval of the manuscript. Galán-Arriola: Supporting in infarct procedure and in CMR images analysis. Critical review of the manuscript. Final approval of the manuscript. Dantas: Planning, design, and analysis of protocols for serum cytokine expression (array) and quantitative real-time PCR. Data interpretation. Critical review of the manuscript. Final approval of the manuscript. Fernández-Friera: Planning and design of imaging protocols (CMR and CT). Blinded analysis of CT images and perfusion CMR images. Data interpretation. Critical review of the manuscript. Final approval of the manuscript. Gálvez-Montón: Immunohistochemical experimentation. Critical review of the manuscript. Final approval of the manuscript. Rigol-Monzó: Analysis and interpretation of flow cytometry crossmatch to detect donor-specific antibodies. Final approval of the manuscript. Agüero: Supporting in infarct procedure. Data interpretation. Final approval of the manuscript. Ramírez: Histopathological studies of the specimens. Data interpretation. Final approval of the manuscript. Roqué: Co-design of study experiments. Critical review of the manuscript. Final approval of the manuscript. Bayés-Genís: Critical review of the manuscript. Final approval of the manuscript. Sánchez-González: CMR imaging protocol and image analysis definition. Critical review of the manuscript. Final approval of the manuscript. García: Planning and design of imaging tests. Blinded analysis of CMR images (cine, T2, and DE sequences). Data interpretation. Critical review of the manuscript. Final approval of the manuscript. Sabaté: Planning and co-design of study experiments. Data interpretation. Handle funding for the study. Critical review of the manuscript. Final approval of the manuscript. Roura: Planning and co-design of study experiments. Cell isolation, expansion, labeling, and sorting. Manuscript writing. Final approval of the manuscript. Ibáñez: Design of the in vivo experiments. Supervision of myocardial infarction, intracoronary delivery of cells/vehicle, and CMR studies execution and analyses. Handle funding for the study. Made critical revision to the manuscript. Final approval of the manuscript. Rigol: Project coordinator. Planning and co-design of study experiments. Subcutaneous adipose tissue collection, infarct procedure, intracoronary administration of cells/vehicle, histological studies. Data interpretation and critical review of the manuscript. Final approval of the manuscript.

Acknowledgments

We thank Ferran Torres, MD, PhD (Medical Statistics Core Facility, IDIBAPS, Hospital Clinic de Barcelona, Barcelona, Spain) for statistical analysis assistance; Nadia Castillo for technical assistance in histological analysis; Gonzalo Javier López-Martín for CMR studies acquisition; and Elaine Lilly for English editing.

Sources of Funding

This work was supported by grants from Fundación la Marató de TV3 (122230); Fondo de Investigación Sanitaria Instituto de Salud Carlos III and Fondo Europeo de Desarrollo Regional (FIS PI14/01682), (RD12/0042/0006), (RD12/0042/0047), (RD12/0019/0029) (TerCel RD16/0011/0006), CIBER

Cardiovascular (CB16/11/00403) projects and Ministerio de Educación y Ciencia (SAF2011-30067-C02-01) (SAF2014-59892). Fernández-Jiménez was the recipient of nonoverlapping grants from the Ministerio de Economía, Industria, y Competitividad through the Instituto de Salud Carlos III (Rio Hortega fellowship); and the Fundación Jesús Serra, the Fundación Interhospitalaria de Investigación Cardiovascular (FIC), and the CNIC (FICNIC fellowship). The use of QMass software was partly supported by a scientific collaboration between the CNIC and Medis Medical Imaging Systems BV. The CNIC is supported by the Ministerio de Economía, Industria, y Competitividad (MINECO) and the Pro CNIC Foundation, and is a Severo Ochoa Center of Excellence (MINECO award SEV-2015-0505). This work was also funded by "la Caixa" Banking Foundation, and the Generalitat de Catalunya (SGR 2014, CERCA Programme). This work has been developed in the context of AdvanceCat with the support of ACCIÓ (Catalonia Trade & Investment; Generalitat de Catalunya) under the Catalonian ERDF operational program (European Regional Development Fund) 2014-2020.

Disclosures

None.

References

1. Behfar A, Crespo-Diaz R, Terzic A, Gersh BJ. Cell therapy for cardiac repair—lessons from clinical trials. *Nat Rev Cardiol*. 2014;11:232–246.
2. Srijaya TC, Ramasamy TS, Kasim NHA. Advancing stem cell therapy from bench to bedside: lessons from drug therapies. *J Transl Med*. 2014;12:243.
3. Jimenez-Quevedo P, Gonzalez-Ferrer JJ, Sabate M, Garcia-Moll X, Delgado-Bolton R, Llorente L, Bernardo E, Ortega-Pozzi A, Hernandez-Antolin R, Alfonso F, Gonzalo N, Escaned J, Bañuelos C, Regueiro A, Marin P, Fernandez-Ortiz A, Das Neves B, Del Trigo M, Fernandez C, Tejerina T, Redondo S, Garcia E, Macaya C. Selected CD133+ progenitor cells to promote angiogenesis in patients with refractory angina final results of the PROGENITOR randomized trial. *Circ Res*. 2014;115:950–960.
4. Bolli R, Chugh AR, D'Amario D, Loughran JH, Stoddard MF, Ikram S, Beache GM, Wagner SG, Leri A, Hosoda T, Sanada F, Elmore JB, Goichberg P, Cappetta D, Solankhi NK, Fahsah I, Rokosh DG, Slaughter MS, Kajstura J, Anversa P. Cardiac stem cells in patients with ischaemic cardiomyopathy (SCIPIO): initial results of a randomised phase 1 trial. *Lancet*. 2011;378:1847–1857.
5. Wang L, Deng J, Tian W, Xiang B, Yang T, Li G, Wang J, Gruwel M, Kashour T, Rendell J, Glogowski M, Tomanek B, Freed D, Deslauriers R, Arora RC, Tian G. Adipose-derived stem cells are an effective cell candidate for treatment of heart failure: an MR imaging study of rat hearts. *Am J Physiol Heart Circ Physiol*. 2009;297:H1020–H1031.
6. Yang J, Yang X, Liu Z, Hu S, Du Z, Feng L, Liu J, Chen Y. Transplantation of adipose tissue-derived stem cells overexpressing heme pxygenase-1 improves functions and remodeling of infarcted myocardium in rabbits. *Tohoku J Exp Med*. 2012;226:231–241.
7. Chen YL, Sun CK, Tsai TH, Chang LT, Leu S, Zhen YY, Sheu JJ, Chua S, Yeh KH, Lu HI, Chang HW, Lee FY, Yip HK. Adipose-derived mesenchymal stem cells embedded in platelet-rich fibrin scaffolds promote angiogenesis, preserve heart function, and reduce left ventricular remodeling in rat acute myocardial infarction. *Am J Transl Res*. 2015;7:781–803.
8. Chen L, Qin F, Ge M, Shu Q, Xu J. Application of adipose-derived stem cells in heart disease. *J Cardiovasc Transl Res*. 2014;7:651–663.
9. Badimon L, Oñate B, Vilahur G. Adipose-derived mesenchymal stem cells and their reparative potential in ischemic heart disease. *Rev Esp Cardiol (Engl Ed)*. 2015;68:599–611.
10. Suzuki E, Fujita D, Takahashi M, Oba S, Nishimatsu H. Adipose tissue-derived stem cells as a therapeutic tool for cardiovascular disease. *World J Cardiol*. 2015;7:454–465.
11. Rigol M, Solanes N, Roura S, Roqué M, Novensà L, Dantas AP, Martorell J, Sitges M, Ramírez J, Bayés-Genís A, Heras M. Allogeneic adipose stem cell therapy in acute myocardial infarction. *Eur J Clin Invest*. 2014;44:83–92.
12. Golpanian S, Rico L, Herrera C. Concise review: bone marrow mononuclear cells for the treatment of ischemic syndromes: medicinal product or cell transplantation? *Stem Cells Transl Med*. 2012;1:403–408.
13. Jansen Of Lorkeers SJ, Eding JEC, Vesterinen HM, Van Der Spoel TIG, Sena ES, Duckers HJ, Doevendans PA, Macleod MR, Chamuleau SAJ. Similar effect of autologous and allogeneic cell therapy for ischemic heart disease: systematic review and meta-analysis of large animal studies. *Circ Res*. 2015;116:80–86.
14. Hare JM, Fishman JE, Gerstenblith G, DiFede Velazquez DL, Zambrano JP, Suncion VY, Tracy M, Ghersin E, Johnston PV, Brinker JA, Breton E, Davis-Sproul J, Schulman IH, Byrnes J, Mendizabal AM, Lowery MH, Rouy D, Altman P, Wong Po Foo C, Ruiz P, Amador A, Da Silva J, McNiece IK, Heldman AW, George R, Lardo A. Comparison of allogeneic vs autologous bone marrow–derived mesenchymal stem cells delivered by transendocardial injection in patients with ischemic cardiomyopathy: the POSEIDON randomized trial. *JAMA*. 2012;308:2369–2379.
15. Rigol M, Solanes N, Farré J, Roura S, Roqué M, Berruezo A, Bellera N, Novensà L, Tamborero D, Prat-Vidal C, Huzman MÁ, Batlle M, Hoefsloot M, Sitges M, Ramírez J, Dantas AP, Merino A, Sanz G, Brugada J, Bayés-Genís A, Heras M. Effects of adipose tissue-derived stem cell therapy after myocardial infarction: impact of the route of administration. *J Card Fail*. 2010;16:357–366.
16. Perea-Gil I, Prat-Vidal C, Gálvez-Montón C, Roura S, Llucià-Valldeperas A, Soler-Botija C, Iborra-Egea O, Díaz-Güemes I, Crisóstomo V, Sánchez-Margallo FM, Bayes-Genis A. A cell-enriched engineered myocardial graft limits infarct size and improves cardiac function. *JACC Basic Transl Sci*. 2016;1:360–372.
17. García-Prieto J, García-Ruiz JM, Sanz-Rosa D, Pun A, García-Álvarez A, Davidson SM, Fernández-Friera L, Nuno-Ayala M, Fernández-Jiménez R, Bernal JA, Izquierdo-Garcia JL, Jimenez-Borreguero J, Pizarro G, Ruiz-Cabello J, Macaya C, Fuster V, Yellon DM, Ibanez B. B3 adrenergic receptor selective stimulation during ischemia/reperfusion improves cardiac function in translational models through inhibition of mPTP opening in cardiomyocytes. *Basic Res Cardiol*. 2014;109:422.
18. Fernández-Jiménez R, Sánchez-González J, Agüero J, García-Prieto J, López-Martín GJ, García-Ruiz JM, Molina-Iracheta A, Rossell X, Fernández-Friera L, Pizarro G, García-Álvarez A, Dall'Armellina E, Macaya C, Choudhury RP, Fuster V, Ibáñez B. Myocardial edema after ischemia/reperfusion is not stable and follows a bimodal pattern: imaging and histological tissue characterization. *J Am Coll Cardiol*. 2015;65:315–323.
19. Fernández-Jiménez R, García-Prieto J, Sánchez-González J, Agüero J, López-Martín GJ, Galán-Arriola C, Molina-Iracheta A, Doohan R, Fuster V, Ibáñez B. Pathophysiology underlying the bimodal edema phenomenon after myocardial ischemia/reperfusion. *J Am Coll Cardiol*. 2015;66:816–828.
20. Ibanez B, Fuster V, Macaya C, Sánchez-Brunete V, Pizarro G, López-Romero P, Mateos A, Jiménez-Borreguero J, Fernández-Ortiz A, Sanz G, Fernández-Friera L, Corral E, Barreiro MV, Ruiz-Mateos B, Goicolea J, Hernández-Antolín R, Acebal C, García-Rubira JC, Albarrán A, Zamorano JL, Casado I, Valenciano J, Fernández-Vázquez F, De La Torre JM, Pérez De Prado A, Iglesias-Vázquez JA, Martínez-Tenorio P, Iñiguez A. Study design for the effect of METOprolol in CARDioproteCtioN during an acute myocardial InfarCtion (METOCARD-CNIC): a randomized, controlled parallel-group, observer-blinded clinical trial of early pre-reperfusion metoprolol administration in ST-segment. *Am Heart J*. 2012;164:473–480.e5.
21. García-Ruiz JM, Fernández-Jiménez R, García-Alvarez A, Pizarro G, Galán-Arriola C, Fernández-Friera L, Mateos A, Nuno-Ayala M, Aguero J, Sánchez-González J, García-Prieto J, López-Melgar B, Martínez-Tenorio P, López-Martín GJ, Macías A, Pérez-Asenjo B, Cabrera JA, Fernández-Ortiz A, Fuster V, Ibáñez B. Impact of the timing of metoprolol administration during STEMI on infarct size and ventricular function. *J Am Coll Cardiol*. 2016;67:2093–2104.
22. Sánchez-González J, Fernandez-Jiménez R, Nothnagel ND, López-Martín G, Fuster V, Ibañez B. Optimization of dual-saturation single bolus acquisition for quantitative cardiac perfusion and myocardial blood flow maps. *J Cardiovasc Magn Reson*. 2015;17:21.
23. Novensa L, Selent J, Pastor M, Sandberg K, Heras M, Dantas AP. Equine estrogens impair nitric oxide production and endothelial nitric oxide synthase transcription in human endothelial cells compared with the natural 17B-estradiol. *Hypertension*. 2010;56:405–411.
24. Makkar RR, Smith RR, Cheng K, Malliaras K, Thomson LEJ, Berman D, Czer LSC, Marbán L, Mendizabal A, Johnston PV, Russell SD, Schuleri KH, Lardo AC, Gerstenblith G, Marbán E. Intracoronary cardiosphere-derived cells for heart regeneration after myocardial infarction (CADUCEUS): a prospective, randomised phase 1 trial. *Lancet*. 2012;379:895–904.

25. Johnston PV, Sasano T, Mills K, Evers R, Lee ST, Smith RR, Lardo AC, Lai S, Steenbergen C, Gerstenblith G, Lange R, Marbán E. Engraftment, differentiation, and functional benefits of autologous cardiosphere-derived cells in porcine ischemic cardiomyopathy. *Circulation*. 2009;120:1075–1083.
26. Gallet R, Tseliou E, Dawkins J, Middleton R, Valle J, Angert D, Reich H, Luthringer D, Kreke M, Smith R, Marban L, Marban E. Intracoronary delivery of self-assembling heart-derived microtissues (cardiospheres) for prevention of adverse remodeling in a pig model of convalescent myocardial infarction. *Circ Cardiovasc Interv*. 2015;8:e002391.
27. Lee HW, Lee HC, Park JH, Kim BW, Ahn J, Kim JH, Park JS, Oh JH, Choi JH, Cha KS, Hong TJ, Park TS, Kim SP, Song S, Kim JY, Park MH, Jung JS. Effects of intracoronary administration of autologous adipose tissue-derived stem cells on acute myocardial infarction in a porcine model. *Yonsei Med J*. 2015;56:1522–1529.
28. Mu D, Zhang X, Xie J, Yuan H, Wang K, Huang W. Intracoronary transplantation of mesenchymal stem cells with overexpressed integrin-linked kinase improves cardiac function in porcine myocardial infarction. *Sci Rep*. 2016;6:19155.
29. Houtgraaf JH, De Jong R, Kazemi K, De Groot D, Van Der Spoel TIG, Arslan F, Hoefer I, Pasterkamp G, Itescu S, Zijlstra F, Geleijnse ML, Serruys PW, Duckers HJ. Intracoronary infusion of allogeneic mesenchymal precursor cells directly after experimental acute myocardial infarction reduces infarct size, abrogates adverse remodeling, and improves cardiac function. *Circ Res*. 2013;113:153–166.
30. Ibáñez B, Heusch G, Ovize M, Van De Werf F. Evolving therapies for myocardial ischemia/reperfusion injury. *J Am Coll Cardiol*. 2015;65:1454–1471.
31. Valina C, Pinkernell K, Song YH, Bai X, Sadat S, Campeau RJ, Le Jemtel TH, Alt E. Intracoronary administration of autologous adipose tissue-derived stem cells improves left ventricular function, perfusion, and remodelling after acute myocardial infarction. *Eur Heart J*. 2007;28:2667–2677.
32. Heiss C, Keymel S, Niesler U, Ziemann J, Kelm M, Kalka C. Impaired progenitor cell activity in age-related endothelial dysfunction. *J Am Coll Cardiol*. 2005;45:1441–1448.
33. Vasa M, Fichtlscherer S, Aicher A, Adler K, Urbich C, Martin H, Zeiher AM, Dimmeler S. Number and migratory activity of circulating endothelial progenitor cells inversely correlate with risk factors for coronary artery disease. *Circ Res*. 2001;89:E1–E7.
34. Kitazawa Y, Li XK, Xie L, Zhu P, Kimur H, Takahara S. Bone marrow-derived conventional, but not cloned, mesenchymal stem cells suppress lymphocyte proliferation and prevent graft-versus-host disease in rats. *Cell Transplant*. 2012;21:581–590.
35. Kanazawa H, Tseliou E, Dawkins JF, De Couto G, Gallet R, Malliaras K, Yee K, Kreke M, Valle I, Smith RR, Middleton RC, Ho C-S, Dharmakumar R, Li D, Makkar RR, Fukuda K, Marban L, Marban E. Durable benefits of cellular postconditioning: long-term effects of allogeneic cardiosphere-derived cells infused after reperfusion in pigs with acute myocardial infarction. *J Am Heart Assoc*. 2016;5:e002796. DOI: 10.1161/JAHA.115.002796.
36. Ock SA, Baregundi Subbarao R, Lee YM, Lee JH, Jeon RH, Lee SL, Park JK, Hwang SC, Rho GJ. Comparison of immunomodulation properties of porcine mesenchymal stromal/stem cells derived from the bone marrow, adipose tissue, and dermal skin tissue. *Stem Cells Int*. 2016;2016:15.
37. Hatzistergos KE, Quevedo H, Oskouei BN, Hu Q, Feigenbaum GS, Margitich IS, Mazhari R, Boyle AJ, Zambrano JP, Rodriguez JE, Dulce R, Pattany PM, Valdes D, Revilla C, Heldman AW, McNiece I, Hare JM. Bone marrow mesenchymal stem cells stimulate cardiac stem cell proliferation and differentiation. *Circ Res*. 2010;107:913–922.
38. Adutler-Lieber S, Ben-Mordechai T, Naftali-Shani N, Asher E, Loberman D, Raanani E, Leor J. Human macrophage regulation via interaction with cardiac adipose tissue-derived mesenchymal stromal cells. *J Cardiovasc Pharmacol Ther*. 2012;18:78–86.
39. Ebrahimi B, Eirin A, Li Z, Zhu X-Y, Zhang X, Lerman A, Textor SC, Lerman LO. Mesenchymal stem cells improve medullary inflammation and fibrosis after revascularization of swine atherosclerotic renal artery stenosis. *PLoS One*. 2013;8:e67474.
40. van den Akker F, Deddens JC, Doevendans PA, Sluijter JPG. Cardiac stem cell therapy to modulate inflammation upon myocardial infarction. *Biochim Biophys Acta*. 2013;1830:2449–2458.
41. Mazo M, Hernández S, Gavira JJ, Abizanda G, Araña M, López-Martínez T, Moreno C, Merino J, Martino-Rodríguez A, Uixeira A, García de Jalón JA, Pastrana J, Martínez-Caro D, Prósper F. Treatment of reperfused ischemia with adipose-derived stem cells in a preclinical swine model of myocardial infarction. *Cell Transplant*. 2012;21:2723–2733.
42. Eirin A, Zhu XY, Krier JD, Tang H, Jordan KL, Grande JP, Lerman A, Textor SC, Lerman LO. Adipose tissue-derived mesenchymal stem cells improve revascularization outcomes to restore renal function in swine atherosclerotic renal artery stenosis. *Stem Cells*. 2012;30:1030–1041.
43. Yang D, Wang W, Li L, Peng Y, Chen P, Huang H, Guo Y, Xia X, Wang Y, Wang H, Wang WE, Zeng C. The relative contribution of paracrine effect versus direct differentiation on adipose-derived stem cell transplantation mediated cardiac repair. *PLoS One*. 2013;8:1–11.
44. Jayasankar V, Woo YJ, Pirolli TJ, Bish LT, Berry MF, Burdick J, Gardner TJ, Sweeney HL. Induction of angiogenesis and inhibition of apoptosis by hepatocyte postischemic heart failure. *J Card Surg*. 2005;20:93–101.
45. Ellison GM, Torella D, Dellegrottaglie S, Perez-Martinez C, Perez De Prado A, Vicinanza C, Purushothaman S, Galuppo V, Iaconetti C, Waring CD, Smith A, Torella M, Cuellas Ramon C, Gonzalo-Orden JM, Agosti V, Indolfi C, Galianes M, Fernandez-Vazquez F, Nadal-Ginard B. Endogenous cardiac stem cell activation by insulin-like growth factor-1/hepatocyte growth factor intracoronary injection fosters survival and regeneration of the infarcted pig heart. *J Am Coll Cardiol*. 2011;58:977–986.
46. Gómez-Mauricio G, Moscoso I, Martín-Cancho M-F, Crisóstomo V, Prat-Vidal C, Báez-Díaz C, Sánchez-Margallo FM, Bernad A. Combined administration of mesenchymal stem cells overexpressing IGF-1 and HGF enhances neovascularization but moderately improves cardiac regeneration in a porcine model. *Stem Cell Res Ther*. 2016;7:94.
47. Mirotsou M, Zhang Z, Deb A, Zhang L, Gnecchi M, Noiseux N, Mu H, Pachori A, Dzau V. Secreted frizzled related protein 2 (Sfrp2) is the key Akt-mesenchymal stem cell-released paracrine factor mediating myocardial survival and repair. *Proc Natl Acad Sci USA*. 2007;104:1643–1648.
48. Voorhees AP, DeLeon-Pennell KY, Ma Y, Halade GV, Yabluchanskiy A, Iyer RP, Flynn E, Cates CA, Lindsey ML, Han H-C. Building a better infarct: modulation of collagen cross-linking to increase infarct stiffness and reduce left ventricular dilation post-myocardial infarction. *J Mol Cell Cardiol*. 2015;85:229–239.
49. Fernández-Jiménez R, Fernández-Friera L, Sánchez-González J, Ibáñez B. Animal models of tissue characterization of area at risk, edema and fibrosis. *Curr Cardiovasc Imaging Rep*. 2014;7:1–10.